



## Luminescence Properties of $\text{Ca}_{1-x}\text{Sr}_x(\text{Ga}_{1-y}\text{Al}_y)_2\text{S}_4:\text{Eu}^{2+}$ and Their Potential Application for White LEDs

Ruijin Yu, Jing Wang,<sup>z</sup> Mei Zhang, Haibin Yuan, Weijia Ding, Yun An, and Qiang Su<sup>z</sup>

MOE Laboratory of Bioinorganic and Synthetic Chemistry, State Key Laboratory of Optoelectronic Materials and Technologies, School of Chemistry and Chemical Engineering, Sun Yat-sen University, Guangdong 510275, China

A series of  $\text{Ca}_{1-x}\text{Sr}_x(\text{Ga}_{1-y}\text{Al}_y)_2\text{S}_4:0.10\text{Eu}^{2+}$  ( $0.0 \leq x \leq 1.0$ ,  $y = 1.0$ ;  $0.0 \leq y \leq 1.0$ ,  $x = 0$ ) phosphors was synthesized by the evacuated sealed quartz ampoule method. X-ray powder diffraction confirmed the formation of the complete solid solutions of  $\text{Ca}_{1-x}\text{Sr}_x\text{Al}_2\text{S}_4:0.10\text{Eu}^{2+}$  and  $\text{Ca}(\text{Ga}_{1-y}\text{Al}_y)_2\text{S}_4:0.10\text{Eu}^{2+}$ . With the Sr(x) and Al(y) content increasing, the emission peaks of  $\text{Ca}_{1-x}\text{Sr}_x\text{Al}_2\text{S}_4:\text{Eu}^{2+}$  and  $\text{Ca}(\text{Ga}_{1-y}\text{Al}_y)_2\text{S}_4:\text{Eu}^{2+}$  show an obvious blueshift in the range of 496–556 nm. A tunable bluish-green to greenish-yellow light can be controlled by simply adjusting the content of Sr(x) in  $\text{Ca}_{1-x}\text{Sr}_x\text{Al}_2\text{S}_4:\text{Eu}^{2+}$  and Al(y) in  $\text{Ca}(\text{Ga}_{1-y}\text{Al}_y)_2\text{S}_4:\text{Eu}^{2+}$ . All the characteristics indicate that the  $\text{Ca}_{1-x}\text{Sr}_x(\text{Ga}_{1-y}\text{Al}_y)_2\text{S}_4:\text{Eu}^{2+}$  solid solution phosphors are good phosphor candidates for white light-emitting diodes (LEDs).

© 2008 The Electrochemical Society. [DOI: 10.1149/1.2966217] All rights reserved.

Manuscript submitted February 25, 2008; revised manuscript received May 2, 2008. Published August 13, 2008.

Luminescence properties of the ternary compounds  $\text{M}^{\text{II}}\text{M}_2^{\text{III}}(\text{S},\text{Se})_4$  doped with various rare-earth ions have been investigated for many years. Photoluminescence (PL) spectra of  $\text{Eu}^{2+}$ - and  $\text{Ce}^{3+}$ -doped  $\text{M}^{\text{II}}\text{Ga}_2\text{S}_4$  were first reported by Peters and Baglio.<sup>1-3</sup> Later, luminescence properties of the  $\text{Eu}^{2+}$ -doped  $\text{MS}-\text{Al}_2\text{S}_3$  ( $\text{M} = \text{Ca}, \text{Sr}, \text{Ba}$ ) thioaluminates were intensively studied by Le Thi.<sup>4</sup> In 1995,  $\text{BaAl}_2\text{S}_4:\text{Eu}^{2+}$  was introduced as a blue-emitting phosphor for full-color electroluminescent (EL) devices and presented excellent EL performance.<sup>5</sup> Thereafter, the iFire Company adopted it as a new blue source and announced a full-color 34 in. thick dielectric EL screen using the color-by-blue technique.<sup>6</sup> In 2003,  $\text{CaAl}_2\text{S}_4:\text{Eu}^{2+}$  was also reported by Nakua as a green-emitting phosphor for EL applications with considerable high luminance of 4200  $\text{cd}/\text{m}^2$  at 260 V.<sup>7</sup>

In addition to EL application, the ternary compounds  $\text{M}^{\text{II}}\text{M}_2^{\text{III}}(\text{S},\text{Se})_4$  have shown another strong potential in phosphor-converted light-emitting diodes (LEDs) for solid-state lighting.  $\text{CaGa}_2\text{S}_4:\text{Eu}^{2+}$  and  $\text{Sr}_2\text{Ga}_2\text{S}_5:\text{Eu}^{2+}$  greenish-yellow phosphors showed a higher luminescent efficiency (120 and 110%, respectively) than commercial yttrium aluminum garnet: $\text{Ce}^{3+}$  phosphor, and they also can be fabricated with blue chips to produce white light.<sup>8,9</sup> To develop new phosphors for white LEDs, an effective approach mentioned in the literature<sup>10</sup> is to obtain solid-solution compounds by adjusting the cations or anions of the host. For example,  $\text{Gd}^{3+}$  can substitute for  $\text{Y}^{3+}$ ,  $\text{Ca}^{2+}$  can substitute for  $\text{Sr}^{2+}$ ,  $\text{Mg}^{2+}$ , or  $\text{Ba}^{2+}$ , and  $\text{Se}^{2-}$  can substitute for  $\text{S}^{2-}$ .<sup>11-13</sup>

Do<sup>14</sup> systematically investigated the influence of composition and crystal structure on the color-tuning properties of  $\text{Sr}_{1-x}\text{Ca}_x\text{Ga}_2\text{S}_4:\text{Eu}^{2+}$  phosphor and found that the color temperature, rendering index, and brightness of three-band white LEDs can be manipulated by adjusting the content of Ca in the  $\text{Sr}_{1-x}\text{Ca}_x\text{Ga}_2\text{S}_4:\text{Eu}^{2+}$  phosphor. In light of the same orthorhombic  $\text{PbGa}_2\text{Se}_4$  structure, we assume that Ca and Sr thioaluminates maybe have similar optical properties to Ca and Sr thioaluminates. Nevertheless, there is little information about the optical properties of  $\text{Ca}_{1-x}\text{Sr}_x(\text{Ga}_{1-y}\text{Al}_y)_2\text{S}_4:\text{Eu}^{2+}$  solid-solution phosphors up to now.

In this study, the aim is to investigate the variation of optical properties with different cation ratios of Ca/Sr and Al/Ga in  $\text{Ca}_{1-x}\text{Sr}_x(\text{Ga}_{1-y}\text{Al}_y)_2\text{S}_4:\text{Eu}^{2+}$  phosphor, including the relative brightness, full width at half-maximum (fwhm), and color coordinates (x, y) based on the 1931 CIE chromaticity diagram.

### Experimental

The starting sulfide materials were pre-prepared by a solid-state reaction method at a high temperature in horizontal tube furnaces. CaS and SrS were prepared from  $\text{CaCO}_3$  [analytical reagent (A.R.)] and  $\text{SrCO}_3$  (A.R.) under flowing  $\text{H}_2\text{S}$  gas at 1000 °C for 2 h.  $\text{Ga}_2\text{S}_3$  was prepared from  $\text{Ga}_2\text{O}_3$  (A.R.) under flowing  $\text{H}_2\text{S}$  gas at 950 °C for 2 h. EuS was prepared from  $\text{Eu}_2\text{O}_3$  (99.99%) with  $\text{CS}_2$  reducing atmosphere at 1200 °C for 3 h.

In order to obtain  $\text{Ca}_{1-x}\text{Sr}_x(\text{Ga}_{1-y}\text{Al}_y)_2\text{S}_4:0.10\text{Eu}^{2+}$  ( $0.0 \leq x \leq 1.0$ ,  $y = 1.0$ ;  $0.0 \leq y \leq 1.0$ ,  $x = 0$ ) phosphors, the stoichiometric amounts of the starting materials CaS, SrS,  $\text{Ga}_2\text{S}_3$ , Al (A.R.), EuS, and 25 mass % excess S (A.R.) were thoroughly mixed and put in the quartz ampoules, evacuated to  $1 \times 10^{-6}$  Torr and sealed, and finally fired at 1050 °C for 5 h.

The structure of the final products was examined using a Rigaku D/max 2200 vpc X-ray diffractometer with  $\text{Cu K}\alpha$  radiation at 40 kV and 30 mA. The PL and PL excitation spectra of  $\text{Ca}_{1-x}\text{Sr}_x\text{Al}_2\text{S}_4:\text{Eu}^{2+}$  and  $\text{Ca}(\text{Ga}_{1-y}\text{Al}_y)_2\text{S}_4:\text{Eu}^{2+}$  were measured by a Fluorolog-3 spectrofluorometer (Jobin Yvon Inc/specx) equipped with a 450 W Xe lamp and double-excitation monochromators. The above measurements were carried out at room temperature.

### Results and Discussion

X-ray diffraction (XRD) patterns of  $\text{Ca}_{1-x}\text{Sr}_x\text{Al}_2\text{S}_4:0.10\text{Eu}^{2+}$  ( $0.0 \leq x \leq 1.0$ ) and  $\text{Ca}(\text{Ga}_{1-y}\text{Al}_y)_2\text{S}_4:0.10\text{Eu}^{2+}$  ( $0.0 \leq y \leq 1.0$ ) are presented in Fig. 1 and 2. The results show that all these compounds are of a pure phase consistent with corresponding JCPDS cards ( $\text{CaAl}_2\text{S}_4$ : #77-1186;  $\text{SrAl}_2\text{S}_4$ : #77-1188;  $\text{CaGa}_2\text{S}_4$ : #25-0134). The lattice constants of  $\text{CaAl}_2\text{S}_4:0.10\text{Eu}^{2+}$  ( $a = 20.173 \text{ \AA}$ ,  $b = 20.025 \text{ \AA}$ ,  $c = 12.007 \text{ \AA}$ , and  $V = 4850.65 \text{ \AA}^3$ ) are slightly smaller than those of  $\text{CaGa}_2\text{S}_4:0.10\text{Eu}^{2+}$  ( $a = 20.037 \text{ \AA}$ ,  $b = 20.143 \text{ \AA}$ ,  $c = 12.129 \text{ \AA}$ , and  $V = 4895.52 \text{ \AA}^3$ ) and  $\text{SrAl}_2\text{S}_4:0.10\text{Eu}^{2+}$  ( $a = 20.841 \text{ \AA}$ ,  $b = 20.426 \text{ \AA}$ ,  $c = 12.125 \text{ \AA}$ , and  $V = 5161.53 \text{ \AA}^3$ ). Compared with the previous results,<sup>15</sup> lattice constants of the samples obtained can be regarded as reasonable.

With careful comparison of the XRD patterns of the series of samples between  $2\theta$  (29–44°) in Fig. 1b and Fig. 2b, a systematic shift toward lower and higher  $2\theta$  value was observed with increasing amounts of  $\text{Sr}^{2+}$  in the  $\text{Ca}_{1-x}\text{Sr}_x\text{Al}_2\text{S}_4$  and  $\text{Al}^{3+}$  in the  $\text{Ca}(\text{Ga}_{1-y}\text{Al}_y)_2\text{S}_4$  systems, respectively. It can be explained that the substitution of  $\text{Sr}^{2+}$  for  $\text{Ca}^{2+}$  causes an increase in the lattice constants of  $\text{Ca}_{1-x}\text{Sr}_x\text{Al}_2\text{S}_4$  due to the larger radius of  $\text{Sr}^{2+}$  ion, and that of  $\text{Al}^{3+}$  for  $\text{Ga}^{3+}$  leads to a decrease in the lattice constants of  $\text{Ca}(\text{Ga}_{1-y}\text{Al}_y)_2\text{S}_4$  due to the smaller radius of  $\text{Al}^{3+}$  ion. Similar results were reported in the  $\text{Sr}_{1-x}\text{Ca}_x\text{Ga}_2\text{S}_4:\text{Eu}^{2+}$  phosphors,<sup>14</sup> indicating the complete miscibility in the  $\text{Ca}_{1-x}\text{Sr}_x\text{Al}_2\text{S}_4$  and

<sup>z</sup> E-mail: ceswj@mail.sysu.edu.cn; suqiang@mail.sysu.edu.cn

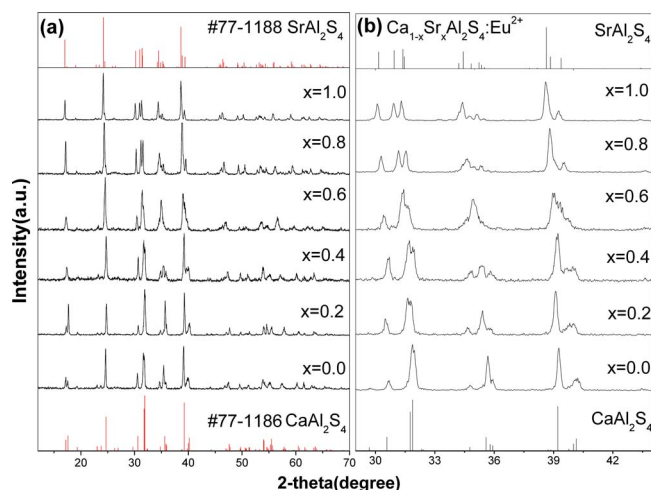


**Figure 1.** (Color online) XRD patterns (a) and local patterns (b) ( $29\text{--}44^\circ$ ) of  $\text{Ca}_{1-x}\text{Sr}_x\text{Al}_2\text{S}_4:0.10\text{Eu}^{2+}$  ( $0.0 \leq x \leq 1.0$ ).

$\text{Ca}(\text{Ga}_{1-y}\text{Al}_y)_2\text{S}_4$  systems in the whole concentration range, and the added  $\text{Eu}^{2+}$  had no influence on the crystal structure of the systems.

Figures 3 and 4 display the PL spectra of  $\text{Eu}^{2+}$  in the  $\text{Ca}_{1-x}\text{Sr}_x\text{Al}_2\text{S}_4$  ( $0.0 \leq x \leq 1.0$ ) and  $\text{Ca}(\text{Ga}_{1-y}\text{Al}_y)_2\text{S}_4$  ( $0.0 \leq y \leq 1.0$ ). It is obvious that all the spectrum features of all phosphors including excitation and emission are similar. The excitation spectra of all the samples consist of two broad bands, the high-energy (250–350 nm) and low-energy (350–500 nm) bands. The broad excitation band makes it well-matched with the emission of UV-LEDs (350–410 nm) and blue-LEDs (430–500 nm). The higher-energy bands are caused by the transitions between the valence and conduction bands of the phosphor hosts. The lower-energy bands are attributed to the  $4f^7 \rightarrow 4f^65d$  transitions of  $\text{Eu}^{2+}$  ions.<sup>16</sup>

By carefully contrasting the excitation spectra (see Fig. 3a and 4a), it can be seen that the absorption bands gradually show blueshift with increasing amounts of Sr ions in the  $\text{Ca}_{1-x}\text{Sr}_x\text{Al}_2\text{S}_4$  and Al ions in the  $\text{Ca}(\text{Ga}_{1-y}\text{Al}_y)_2\text{S}_4$  systems. Accordingly, the normalized emission peaks of samples also show an obvious blueshift behavior (see Fig. 3b and 4b). The emission wavelength is 556 nm for  $\text{CaGa}_2\text{S}_4:0.10\text{Eu}^{2+}$  ( $y = 0.0$ ), 540 nm for  $\text{Ca}(\text{Ga}_{0.6}\text{Al}_{0.4})_2\text{S}_4:0.10\text{Eu}^{2+}$  ( $y = 0.4$ ), 516 nm for  $\text{CaAl}_2\text{S}_4:0.10\text{Eu}^{2+}$  ( $x = 0.0$ ), 504 nm for  $\text{Ca}_{0.6}\text{Sr}_{0.4}\text{Al}_2\text{S}_4:0.10\text{Eu}^{2+}$  ( $x = 0.4$ ), and 496 nm for  $\text{SrAl}_2\text{S}_4:0.10\text{Eu}^{2+}$  ( $x = 1.0$ ). As shown in the inset of Fig. 4b, the

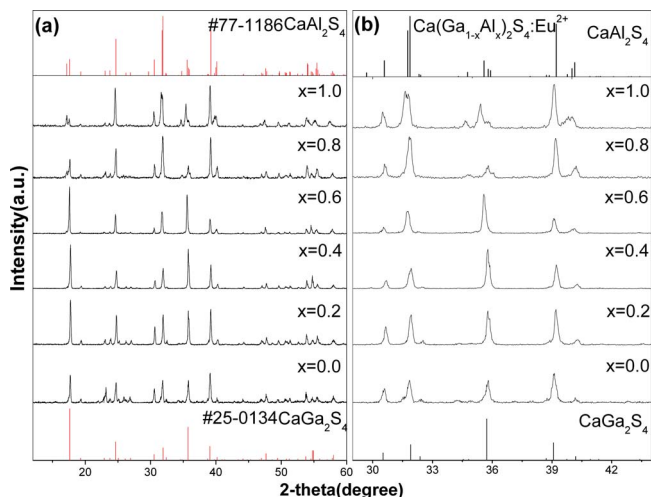


**Figure 2.** (Color online) XRD patterns (a) and local patterns (b) ( $29\text{--}44^\circ$ ) of  $\text{Ca}(\text{Ga}_{1-y}\text{Al}_y)_2\text{S}_4:0.10\text{Eu}^{2+}$  ( $0.0 \leq y \leq 1.0$ ).

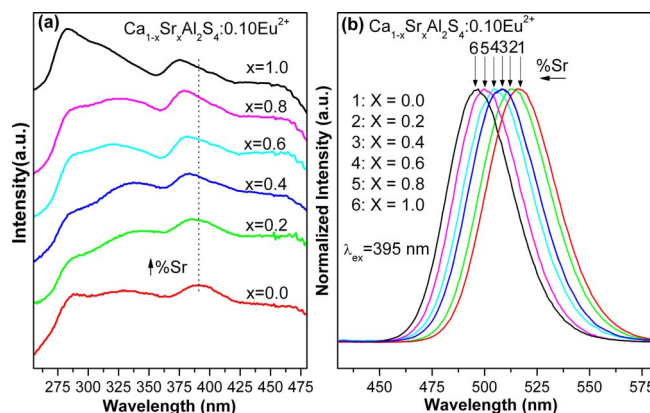


**Figure 3.** (Color online) The excitation (a) and normalized emission (b) spectra of  $\text{Ca}_{1-x}\text{Sr}_x\text{Al}_2\text{S}_4:0.10\text{Eu}^{2+}$  ( $0.0 \leq x \leq 1.0$ ).

emission peaks of  $\text{Ca}(\text{Ga}_{1-y}\text{Al}_y)_2\text{S}_4:\text{Eu}^{2+}$  shift almost linearly to a shorter wavelength with an increase in  $y$ , from 556 nm ( $y = 0.0$ ) to 516 nm ( $y = 1.0$ ).

This shift phenomenon often appears in  $\text{Eu}^{2+}$ -doped solid solution, such as  $\text{Sr}_{4-x}\text{Mg}_x\text{Si}_3\text{O}_8\text{Cl}_4:\text{Eu}^{2+}$ ,  $(\text{Ca}_x\text{Sr}_{1-x})_2\text{Si}_5\text{N}_8:\text{Eu}^{2+}$ ,  $\text{Ca}_{1-x}\text{Sr}_x(\text{S}_y\text{Se}_{1-y})_2:\text{Eu}^{2+}$ , etc.<sup>13,17,18</sup> The blueshift of emission peaks in  $\text{Ca}_{1-x}\text{Sr}_x\text{Al}_2\text{S}_4:\text{Eu}^{2+}$  can be explained in terms of crystal-field strength dependence of the 5d excited level of  $\text{Eu}^{2+}$  ion. When  $\text{Eu}^{2+}$  is doped into  $\text{Ca}_{1-x}\text{Sr}_x\text{Al}_2\text{S}_4$  compounds, it occupies the  $\text{M}^{2+}$  cation sites. The average distance of an Sr–S bond in  $\text{SrAl}_2\text{S}_4$  is 3.072 Å, longer than a Ca–S bond (2.992 Å) in  $\text{CaAl}_2\text{S}_4$ .<sup>15</sup> The distance between the  $\text{Eu}^{2+}$  ion and  $\text{S}^{2-}$  ions increases with the increasing amounts of Sr ions in  $\text{Ca}_{1-x}\text{Sr}_x\text{Al}_2\text{S}_4$ . This makes  $\text{Eu}^{2+}$  ions in  $\text{Ca}_{1-x}\text{Sr}_x\text{Al}_2\text{S}_4$  gradually suffer a weaker crystal field. So, the lowest component of the  $4f^65d$  configuration of the  $\text{Eu}^{2+}$  ion may shift to high energy, which should result in the blueshift behavior of the emission peaks.

Furthermore, the blueshift of emission peaks in  $\text{Ca}(\text{Ga}_{1-y}\text{Al}_y)_2\text{S}_4:\text{Eu}^{2+}$  is mainly due to the centroid shift of the 5d excited level of  $\text{Eu}^{2+}$  ion.  $\text{Al}^{3+}$  and  $\text{Ga}^{3+}$  ions are the so-called counter-cations that polarize or even bind the anion ligands. A strong polarization or bonding goes at the expense of the interaction between the anion and the 5d electron of  $\text{Eu}^{2+}$ .<sup>19</sup> Replacing  $\text{Ga}^{3+}$  by the same valency and smaller  $\text{Al}^{3+}$  leads to the increase in effective electronegativity of the counter-cations and the binding of anion ligands. Therefore, both decrease in anion polarizability and covalency between anion and  $\text{Eu}^{2+}$  lead to smaller centroid shift. A smaller centroid shift tends to result in the blueshift behavior of the emission peaks.

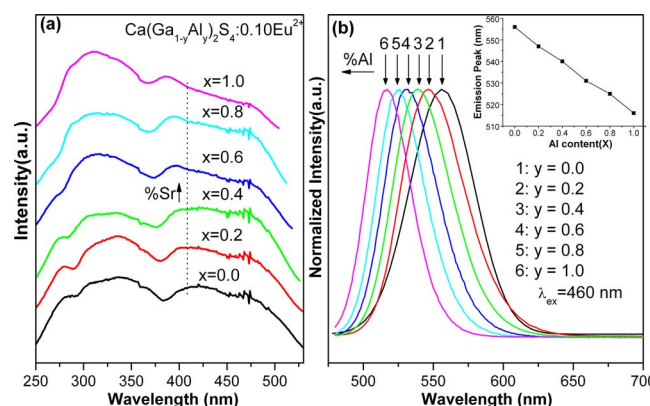


**Figure 4.** (Color online) The excitation (a) and normalized emission (b) spectra of  $\text{Ca}(\text{Ga}_{1-y}\text{Al}_y)_2\text{S}_4:0.10\text{Eu}^{2+}$ . The inset represents the dependence of emission peak on the Al content ( $y$ ) ( $0.0 \leq y \leq 1.0$ ) ( $\lambda_{\text{ex}} = 460$  nm).

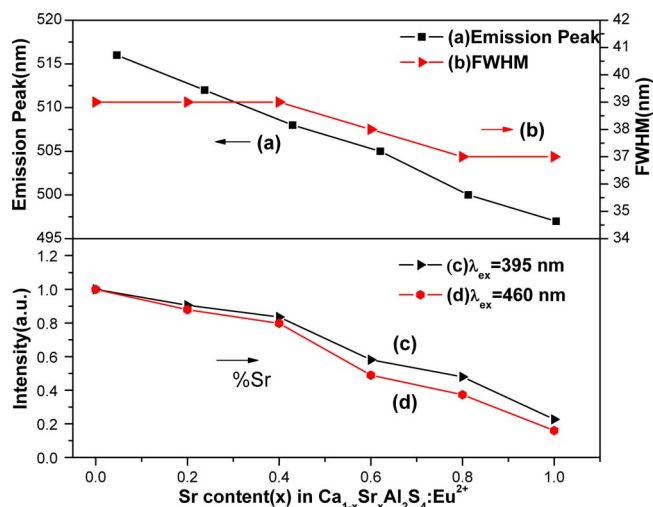


**Figure 5.** (Color online) The dependence of emission peak (a), fwhm (b) and relative intensity [(c):  $\lambda_{ex} = 395$  nm, (d):  $\lambda_{ex} = 460$  nm] on Sr content (x) in  $\text{Ca}_{1-x}\text{Sr}_x\text{Al}_2\text{S}_4:0.10\text{Eu}^{2+}$ .

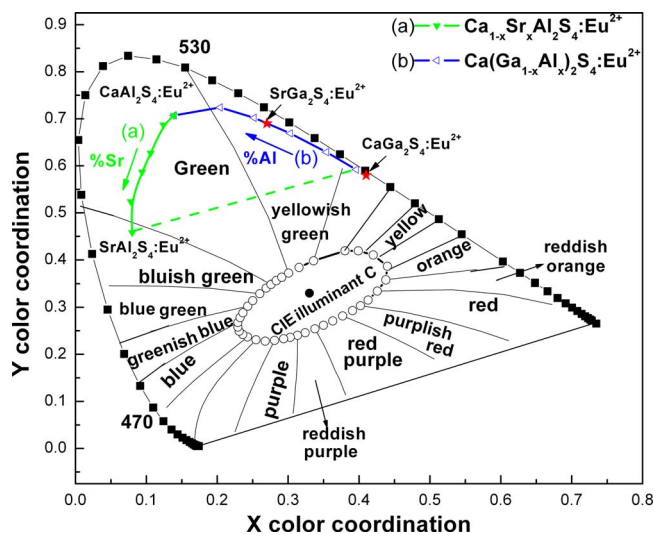
The dependence of emission peak, fwhm, and relative intensity on the Sr content (x) in  $\text{Ca}_{1-x}\text{Sr}_x\text{Al}_2\text{S}_4:0.10\text{Eu}^{2+}$  is shown in Fig. 5. As shown in curve a, the emission peak of  $\text{Ca}_{1-x}\text{Sr}_x\text{Al}_2\text{S}_4:0.10\text{Eu}^{2+}$  also shows a linear blueshift with an increase in x, from 516 nm ( $x = 0.0$ ) to 496 nm ( $x = 1.0$ ). One can achieve a tuning-emission color range of about 19 nm in  $\text{Ca}_{1-x}\text{Sr}_x\text{Al}_2\text{S}_4:0.10\text{Eu}^{2+}$ . Thus, a broad tunable emission color can be achieved in the range of 496–556 nm in  $\text{Ca}_{1-x}\text{Sr}_x(\text{Ga}_{1-y}\text{Al}_y)_2\text{S}_4:\text{Eu}^{2+}$ . The fwhm values are in the range of 39–37 nm. Compared with the common value of fwhm, 50–100 nm, of  $\text{Eu}^{2+}$  ions in most phosphors, these values are smaller in our case, indicating weak interaction of  $\text{Eu}^{2+}$  ions with the host material,  $\text{Ca}_{1-x}\text{Sr}_x\text{Al}_2\text{S}_4$ . In lighting field, the smaller fwhm of emission band is helpful for high luminous output.<sup>20</sup> Curves c and d represent the emission intensities with increasing Sr content under 395 and 460 nm excitation. As can be seen, the emission intensities of the phosphors are higher under 395 nm excitation than those under 460 nm excitation. The emission intensity decreases with increasing Sr content until it reaches about 23 and 16% of  $\text{CaAl}_2\text{S}_4:0.10\text{Eu}^{2+}$  under 395 and 460 nm excitation, respectively.

Figure 6 displays the CIE chromaticity diagram of  $\text{Ca}_{1-x}\text{Sr}_x\text{Al}_2\text{S}_4:0.10\text{Eu}^{2+}$  and  $\text{Ca}(\text{Ga}_{1-y}\text{Al}_y)_2\text{S}_4:0.10\text{Eu}^{2+}$ . The color coordinates of  $\text{CaGa}_2\text{S}_4:\text{Eu}^{2+}$  and  $\text{SrGa}_2\text{S}_4:\text{Eu}^{2+}$  are depicted in the form of pentagrams according to the values reported in Ref. 14. The color coordinates of  $\text{Ca}(\text{Ga}_{1-y}\text{Al}_y)_2\text{S}_4:\text{Eu}^{2+}$  gradually shift from greenish yellow to green along curve b with increasing content of Al(y). Subsequently, the color coordinates of  $\text{Ca}_{1-x}\text{Sr}_x\text{Al}_2\text{S}_4:\text{Eu}^{2+}$  gradually shift into bluish green along curve a with increasing content of Sr(x). Due to their broad color-tunable PL feature, it is meaningful that the appropriate colors can be tailored by controlling the content of Sr(x) in  $\text{Ca}_{1-x}\text{Sr}_x\text{Al}_2\text{S}_4:\text{Eu}^{2+}$  and Al(y) in  $\text{Ca}(\text{Ga}_{1-y}\text{Al}_y)_2\text{S}_4:\text{Eu}^{2+}$ . All the characteristics indicate that  $\text{Ca}_{1-x}\text{Sr}_x(\text{Ga}_{1-y}\text{Al}_y)_2\text{S}_4:\text{Eu}^{2+}$  could be good bluish-green to greenish-yellow phosphor candidates for white LEDs.

It is also reasonable to expect that any color within the quadrilateral region ( $\text{CaGa}_2\text{S}_4$ – $\text{SrGa}_2\text{S}_4$ – $\text{CaAl}_2\text{S}_4$ – $\text{SrAl}_2\text{S}_4$ ) can be easily realized if one controls the content of Sr(x) and Al(y) in  $\text{Ca}_{1-x}\text{Sr}_x(\text{Ga}_{1-y}\text{Al}_y)_2\text{S}_4:\text{Eu}^{2+}$  ( $0 \leq x \leq 1$ ,  $0 \leq y \leq 1$ ). Further research is being carried on.

### Conclusions

In summary, a series of  $\text{Ca}_{1-x}\text{Sr}_x(\text{Ga}_{1-y}\text{Al}_y)_2\text{S}_4:0.10\text{Eu}^{2+}$  ( $0.0 \leq x \leq 1.0$ ,  $y = 1.0$ ;  $0.0 \leq y \leq 1.0$ ,  $x = 0$ ) phosphors were synthesized by the evacuated sealed quartz ampoule method. Their crystal



**Figure 6.** (Color online) The CIE chromaticity diagram of  $\text{Ca}_{1-x}\text{Sr}_x\text{Al}_2\text{S}_4:0.10\text{Eu}^{2+}$  (a,  $\lambda_{ex} = 395$  nm) and  $\text{Ca}(\text{Ga}_{1-y}\text{Al}_y)_2\text{S}_4:0.10\text{Eu}^{2+}$  (b,  $\lambda_{ex} = 460$  nm).

structure and optical properties were also investigated. With the Sr(x) and Al(y) content increasing, the emission peaks of  $\text{Ca}_{1-x}\text{Sr}_x\text{Al}_2\text{S}_4:\text{Eu}^{2+}$  and  $\text{Ca}(\text{Ga}_{1-y}\text{Al}_y)_2\text{S}_4:\text{Eu}^{2+}$  show an obvious blueshift. A broad tunable emission with suitable peak position and color coordinates in the range of 496–556 nm were achieved by adjusting the content of Sr(x) in  $\text{Ca}_{1-x}\text{Sr}_x\text{Al}_2\text{S}_4:\text{Eu}^{2+}$  and Al(y) in  $\text{Ca}(\text{Ga}_{1-y}\text{Al}_y)_2\text{S}_4:\text{Eu}^{2+}$  phosphors. All the characteristics indicate that  $\text{Ca}_{1-x}\text{Sr}_x(\text{Ga}_{1-y}\text{Al}_y)_2\text{S}_4:\text{Eu}^{2+}$  solid-solution phosphors are good phosphor candidates for white LEDs.

### Acknowledgments

This work was supported by the National Nature Science Foundation of China (20501023), the Nature Science Foundation of Guangdong for Doctorial Training base (5300527), and the Science and Technology Project of Guangzhou (2005Z2-D0061).

Sun Yat-sen University assisted in meeting the publication costs of this article.

### References

1. T. E. Peters and J. A. Baglio, *J. Electrochem. Soc.*, **119**, 230 (1972).
2. T. E. Peters, *J. Electrochem. Soc.*, **119**, 1720 (1972).
3. T. E. Peters, *J. Electrochem. Soc.*, **122**, 98 (1975).
4. K. T. Le Thi, A. Garcia, F. Guillen, and C. Fouassier, *Mater. Sci. Eng., B*, **14**, 393 (1992).
5. N. Miura, M. Kawanishi, H. Matsumoto, and R. Nakano, *Jpn. J. Appl. Phys., Part 2*, **38**, L1291 (1999).
6. X. Wu, A. Nakua, and D. Cheong, *J. Soc. Inf. Disp.*, **12**, 281 (2004).
7. A. Nakua, D. Cheong, and X. Wu, *J. Soc. Inf. Disp.*, **11**, 493 (2003).
8. J. M. Kim, K. N. Kim, S. H. Park, J. K. Park, C. H. Kim, and H. G. Jang, *J. Korean Chem. Soc.*, **49**, 201 (2005).
9. J. M. Kim, J. K. Park, K. N. Kim, S. J. Lee, C. H. Kim, and H. G. Jang, *J. Korean Chem. Soc.*, **50**, 2371 (2006).
10. W. J. Ding, J. Wang, M. Zhang, Q. H. Zhang, and Q. Su, *Chem. Phys. Lett.*, **435**, 301 (2007).
11. K. N. Kim, J. K. Park, K. J. Choi, J. M. Kim, and C. H. Kim, *Electrochem. Solid-State Lett.*, **9**, G262 (2006).
12. X. M. Zhang, L. F. Liang, J. H. Zhang, and Q. Su, *Mater. Lett.*, **59**, 749 (2005).
13. M. Nazarov and C. Yoon, *J. Solid J. Solid State Chem.*, **179**, 2529 (2006).
14. Y. R. Do, K. Y. Ko, S. H. Na, and Y. D. Huh, *J. Electrochem. Soc.*, **153**, H142 (2006).
15. B. Eisenmann, M. Jakowski, W. Klee, and H. Schafer, *Rev. Chim. Miner.*, **20**, 255 (1983).
16. J. E. Van Haecke, P. F. Smet, and D. Poelman, *J. Lumin.*, **126**, 50 (2007).
17. T. Jüstel, H. Nikol, and C. Ronda, *Angew. Chem., Int. Ed.*, **37**, 3084 (1998).
18. P. Benalloul, C. Barthou, and J. Benoit, *J. Alloys Compd.*, **275–277**, 709 (1998).
19. P. Dorenbos, *J. Lumin.*, **104**, 239 (2003).
20. X. Piao, T. Horikawa, H. Hanzawa, and K. I. Machida, *J. Electrochem. Soc.*, **153**, H232 (2006).